

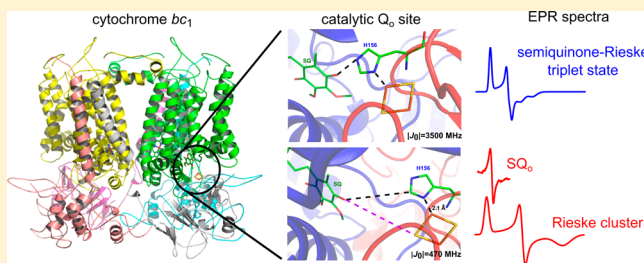
Triplet State of the Semiquinone–Rieske Cluster as an Intermediate of Electronic Bifurcation Catalyzed by Cytochrome bc_1

Marcin Sarewicz, Małgorzata Dutka, Sebastian Pintscher, and Artur Osyczka*

Department of Molecular Biophysics, Faculty of Biochemistry, Biophysics and Biotechnology, Jagiellonian University, Kraków, Poland

S Supporting Information

ABSTRACT: Efficient energy conversion often requires stabilization of one-electron intermediates within catalytic sites of redox enzymes. While quinol oxidoreductases are known to stabilize semiquinones, one of the famous exceptions includes the quinol oxidation site of cytochrome bc_1 (Q_o), for which detection of any intermediate states is extremely difficult. Here we discover a semiquinone at the Q_o site (SQ_o) that is coupled to the reduced Rieske cluster (FeS) via spin–spin exchange interaction. This interaction creates a new electron paramagnetic resonance (EPR) transitions with the most prominent $g = 1.94$ signal shifting to 1.96 with an increase in the EPR frequency from X- to Q-band. The estimated value of isotropic spin–spin exchange interaction ($|J_0| = 3500$ MHz) indicates that at a lower magnetic field (typical of X-band) the SQ_o –FeS coupled centers can be described as a triplet state. Concomitantly with the appearance of the SQ_o –FeS triplet state, we detected a $g = 2.0045$ radical signal that corresponded to the population of unusually fast-relaxing SQ_o for which spin–spin exchange does not exist or is too small to be resolved. The $g = 1.94$ and $g = 2.0045$ signals reached up to 20% of cytochrome bc_1 monomers under aerobic conditions, challenging the paradigm of the high reactivity of SQ_o toward molecular oxygen. Recognition of stable SQ_o reflected in $g = 1.94$ and $g = 2.0045$ signals offers a new perspective on understanding the mechanism of Q_o site catalysis. The frequency-dependent EPR transitions of the SQ_o –FeS coupled system establish a new spectroscopic approach for the detection of SQ_o in mitochondria and other bioenergetic systems.



Biological energy conversion faces an engineering problem of joining the one- and two-electron stoichiometry of redox reactions between substrates and cofactors. Most catalytic sites accomplish this by supporting two sequential one-electron transfers toward a single cofactor chain involving a stable intermediate radical.^{1,2} The catalytic Q_o site of cytochrome bc_1 (respiratory complex III) is different and unique in that it changes the electronic stoichiometry by steering two electrons from ubiquinol (QH_2) to two separate chains of cofactors: it delivers one electron to the Rieske cluster (FeS) in the high-potential chain and the second electron to heme b_L in the low-potential chain (Figure S1 of the Supporting Information).^{3–6} The common view of this bifurcation process is that the intermediate semiquinone radical (SQ_o), formed by one-electron oxidation of QH_2 by FeS, is highly unstable^{5,7} and reduces heme b_L very rapidly before it can react with dioxygen to generate superoxide.^{8–11} This concept has been supported by a general difficulty to detect SQ_o under aerobic conditions. In fact, the only report of detection of SQ_o under those conditions comes from early studies with submitochondrial particles (SOM).¹² The origin of this signal was, however, questioned by later studies showing the insensitivity of the SQ signals in SOM to specific inhibitors of the Q_o site.¹³ More recent studies reported either detection of small amounts of SQ_o under anaerobic conditions^{14,15} or a lack of detection of SQ_o under aerobic conditions,¹⁶ which further supported the concept of the high instability of SQ_o and its high reactivity

with oxygen. Apart from those examples, there have been no other studies reporting detection of intermediate states for Q_o site catalysis, which leaves the mechanism of electronic bifurcation largely unknown.

Here, we explore a possibility that the intriguing lack of SQ_o detection is a result of its magnetic interactions with metal centers of the Q_o site rather than an effect of its high instability. In principle, a strong antiferromagnetic coupling of SQ_o with a metal center could result in the elimination of the SQ_o electron paramagnetic resonance (EPR) signal, as proposed by Link.¹⁷ However, if the coupling is ferromagnetic and/or weak (in comparison to the thermal energy of the lattice), it may be expected that it will manifest itself as a new spectroscopic identity.^{18,19} Indeed, by exposing the purified enzyme to its substrates (oxidized cytochrome c and QH_2), we have detected new transitions in EPR spectra assigned to a SQ_o magnetically coupled to reduced FeS via spin–spin exchange interaction. We also detected a separate radical signal of SQ_o with relaxation properties consistent with its location between the metal centers of the Q_o site. This discovery offers a new perspective on understanding the mechanism of quinol oxidation at the Q_o site. It also provides new insight into side reactions of the

Received: May 17, 2013

Revised: July 18, 2013

Published: August 13, 2013

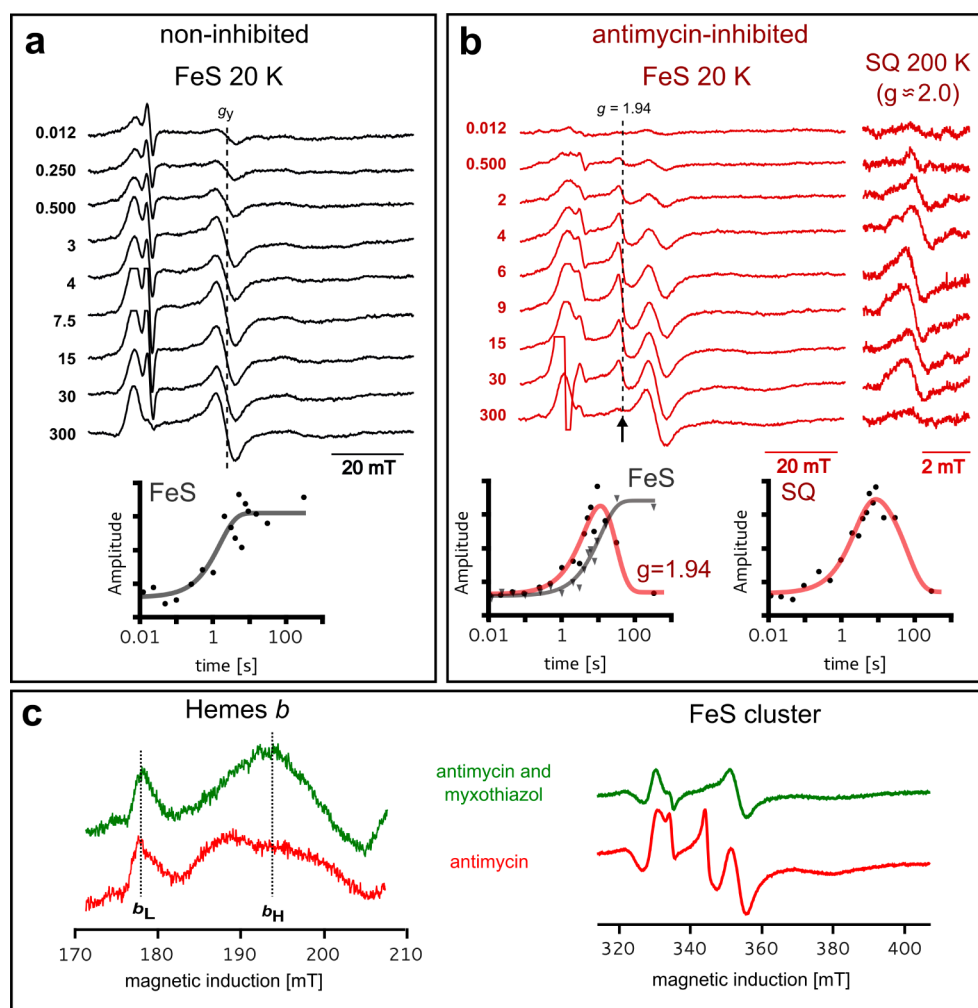


Figure 1. Detection of new $g = 1.94$ and $g = 2.0$ EPR transitions in cytochrome bc_1 . Monitoring changes in paramagnetic states of redox centers in WT cytochrome bc_1 by X-band EPR during steady-state reduction of cytochrome c and oxidation of DBH_2 . Samples were frozen at different time points after addition of DBH_2 to the mixture containing enzyme and cytochrome c . (a) Spectra of FeS in the noninhibited enzyme and time dependence of the amplitude (measured for the g_y transition of FeS indicated by the dashed line). (b) Appearance of a new $g = 1.94$ transition (arrow) and a $g = 2.0$ radical signal in the antimycin-inhibited enzyme. The plot on the left shows time dependencies of the amplitude of the $g = 1.94$ signal (red line) and of g_y of the FeS cluster (gray line). The plot on the right shows the time dependence of the amplitude of the $g = 2.0$ signal. (c) Spectra of hemes b_L and b_H (left) and FeS (right) for mixtures with antimycin-inhibited (red) or myxothiazol- and antimycin-inhibited cytochrome bc_1 (green), respectively, frozen 12 s after addition of DBH_2 . Hemes, FeS, and SQ signals were measured at 10, 20, and 200 K, respectively. In panels a and b, the numbers on the left correspond to the reaction time in seconds (time before freezing).

catalytic cycle involved in the production of superoxide by cytochrome bc_1 .

MATERIALS AND METHODS

Biochemical Procedures. The cytochrome bc_1 complex was isolated from the purple bacterium *Rhodospirillum rubrum* strain grown semiaerobically as described previously.²⁰ Bovine cytochrome c , 2,3-dimethoxy-5-decyl-6-methyl-1,4-benzoquinone (DB), and inhibitors (antimycin, myxothiazol, atovaquone, azoxystrobin, kresoxim-methyl, and famoxadone) were purchased from Sigma-Aldrich and used without further purifications. Tridecyl-stigmatellin was a generous gift from N. Fisher. DB was dissolved in an HCl/DMSO solution and then reduced to its hydroquinone form (DBH_2) with sodium borohydride. Inhibitors were used in 5-fold molar excess over the concentration of cytochrome bc_1 monomers. Cytochrome bc_1 and cytochrome c solutions were dialyzed against the reaction buffer composed of 50 mM Tris (pH 8.0), 100 mM

NaCl, 20% glycerol (v/v), 0.01% (m/m) dodecyl maltoside, and 1 mM EDTA. All buffers were in equilibrium with air. Glycerol, added as a cryoprotective agent, increased the viscosity of the reaction buffer, which resulted in a deceleration of the overall catalytic turnover rate of the enzyme by decreasing diffusion rates of the substrates.

Freeze-quench experiments were performed using a Biologic SFM-300 stopped-flow mixer equipped with an MPS-70 programmable syringe control. The system was equipped with EPR FQ accessories. One syringe contained a cytochrome bc_1 /cytochrome c solution, and the second syringe contained DBH_2 in reaction buffer. Steady-state reduction of cytochrome c by cytochrome bc_1 was initiated by mixing the cytochrome bc_1 /cytochrome c solution with DBH_2 in a 1:1 volume ratio to obtain final concentrations of cytochrome bc_1 , cytochrome c , and DBH_2 of 50, 393, and 665 μ M, respectively. The reaction mixture was incubated at room temperature in a delay line for a programmed number of milliseconds and then injected into an isopentane bath cooled to 100 K. Samples with higher

cytochrome bc_1 concentrations required for hemes b measurements were prepared by manual injection of DBH_2 into the cytochrome bc_1 /cytochrome c solution inside EPR tube. The reaction was stopped by immersing the tube into cold ethanol glue.

EPR Spectroscopy and Data Analysis. All measurements were performed using a Bruker Elexsys ES80 spectrometer. X-Band continuous wave electron paramagnetic resonance (CW EPR) spectra of hemes and FeS were measured at 10 and 20 K, respectively, using a SHQE0511 resonator and ESR900 cryostat (Oxford Instruments). X-Band spectra of semiquinones were recorded using a TM9103 resonator equipped with a temperature controller system (Bruker). Q-Band spectra of semiquinones were measured at 200 K by CW EPR using an ER507D2 resonator (Bruker) equipped with homemade modulation coils using a 0.6 mT modulation amplitude, a 90 kHz frequency, and a 1.92 mW microwave power. Q-Band echo-detected EPR (ED EPR) spectra of FeS were measured at 10 K using a $\pi/2$ –148 ns– π sequence with a π pulse of 48 ns and a shot repetition time of 300 μ s. First-derivative spectra of FeS were generated by applying the pseudomodulation procedure²¹ on ED EPR spectra using Eleana (<http://www.wbbib.uj.edu.pl/web/gbm/eleana>). The magnitude of the external magnetic field was controlled using a Bruker NMR teslameter.

The microwave power saturation profiles of semiquinones were fit using formulas described in ref 22. The data for chemically induced semiquinone (SQ_{CH}) were fit assuming a contribution from one saturable component, while data for SQ_o were fit assuming the presence of two species: major, nonsaturable component and minor, saturable component. The temperature dependencies of the amplitude of SQ_{CH} were fit with the well-known Curie law. The data for SQ_o were fit assuming the presence of the Leigh effect²³ in which the correlation time of the fluctuating dipolar field increases with a decrease in temperature. Q-Band spectra of semiquinones were simulated with Easy-spin²⁴ using the anisotropic g tensor, assuming homogeneous and inhomogeneous line broadening.

Spectral simulations based on a spin Hamiltonian including Zeeman interaction of spins of FeS and SQ_o centers with the external static magnetic field and a general bilinear spin–spin interaction term were performed as described in the Supporting Information.

RESULTS

Detection of New EPR Transitions Associated with the Q_o Site of Cytochrome bc_1 . In searching for intermediates of the Q_o site, we performed series of experiments in which isolated cytochrome bc_1 in equilibrium with air catalyzed steady-state electron transfer from the water-soluble QH_2 analogue [2,3-dimethoxy-5-decyl-6-methyl-1,4-benzohydroquinone (DBH_2)] to oxidized cytochrome c , and the time course of spin states of redox centers was monitored by EPR. The time points of freezing the samples were selected to cover the range from the beginning of the reaction until an equilibrium between the substrates and the products was reached. As a measure of the reaction progress, the amount of oxidized cytochrome c available for reaction was determined from the amplitude of the EPR signal of heme c (not shown). We compared two cases: the reaction catalyzed by the noninhibited enzyme and that catalyzed by the enzyme inhibited with antimycin. These two cases differ by the way in which the heme b_L undergoes reoxidation (after its initial reduction by an electron derived

from quinol) to support the turnover of the Q_o site. In the noninhibited enzyme, heme b_H rapidly reoxidizes heme b_L and then transfers an electron to the Q_i site (see Figure S1 of the Supporting Information). This reaction sequence continues until the equilibrium is reached (the substrates are used up). In the antimycin-inhibited enzyme, the Q_i site is blocked by the inhibitor, and after the first QH_2 oxidation at the Q_o site, heme b_H remains reduced, preventing fast reoxidation of heme b_L after the oxidation of a second QH_2 at the Q_o site. Nevertheless, this heme can undergo slow reoxidation by the back electron transfer to SQ_o that re-forms QH_2 ²⁵ or electron transfer to Q that forms SQ_o .^{5,26–28} With these reactions, the Q_o site can also keep the turnover until the equilibrium is reached, although the overall rate is significantly slower than that of the noninhibited enzyme.

As shown in Figure 1a, in the noninhibited enzyme, the level of reduced FeS increased within the first 7 s, reflecting the expected progress of the reaction, and after an equilibrium had been reached, the amplitude of the FeS signal remained constant. In the antimycin-inhibited enzyme, the rate of reaching the equilibrium level of reduced FeS decreased, as expected, but at the same time, quite unexpectedly we observed an additional EPR transition at $g = 1.94$ (Figure 1b). Its amplitude reached a maximum at 10 s and then gradually decreased to zero. A comparison of amplitudes of EPR signals of hemes b shown in Figure 1c indicates that in the samples exhibiting a $g = 1.94$ signal, heme b_L remained fully oxidized. The presence of a $g = 1.94$ signal correlated with the presence of another weak signal of organic radical at $g = 2.0$ (exact value of 2.0045) detected with the use of a high microwave power (Figure 1b). Both $g = 1.94$ and $g = 2.0$ signals arose during the enzymatic turnover to reach their maximal amplitudes at the time where the g_y (1.89) transition of reduced FeS reached approximately half of its maximal amplitude. After the maximum had been reached, the amplitude of both $g = 1.94$ and $g = 2.0$ signals gradually decreased, and when the system reached equilibrium (g_y of FeS remains at its maximum), both signals disappeared completely.

The experiments described in Figures 1c and 2 asserted that $g = 1.94$ and $g = 2.0$ signals originate specifically from the Q_o site. Both signals were sensitive to inhibitors of the Q_o site and to point mutations that abolish the activity of the site^{7,29} and were not present in the bc_1 subcomplex lacking the FeS subunit.²⁰ On the other hand, the amplitude of the $g = 1.94$ and $g = 2.0$ signals was larger in the mutants with affected motion of the FeS head domain (+2Ala)³⁰ (see Figure S2 of the Supporting Information). As +2Ala arrests this domain at the Q_o site for seconds with FeS in the reduced state³⁰ (this way it abolishes the natural submillisecond electronic connection between the Q_o site and heme c_1), the observed enhancement of the signals immediately suggests that they must be associated with paramagnetism of FeS occupying the Q_o site. Furthermore, in light of all of the results described above, the $g = 2.0$ signal must report SQ_o . We note that $g = 1.94$ and $g = 2.0$ signals were not present in samples reduced with dithionite (not shown), precluding the possibility that they originate from a contamination of the sample with low-potential iron–sulfur centers.

Identification of the Semiquinone–Rieske Cluster Coupled System. Chemicals, such as DMSO or glycerol, and some point mutations have been reported to induce small changes in the EPR spectra of iron–sulfur clusters in proteins (Rieske or ferredoxins) with shifts in the g_y values of

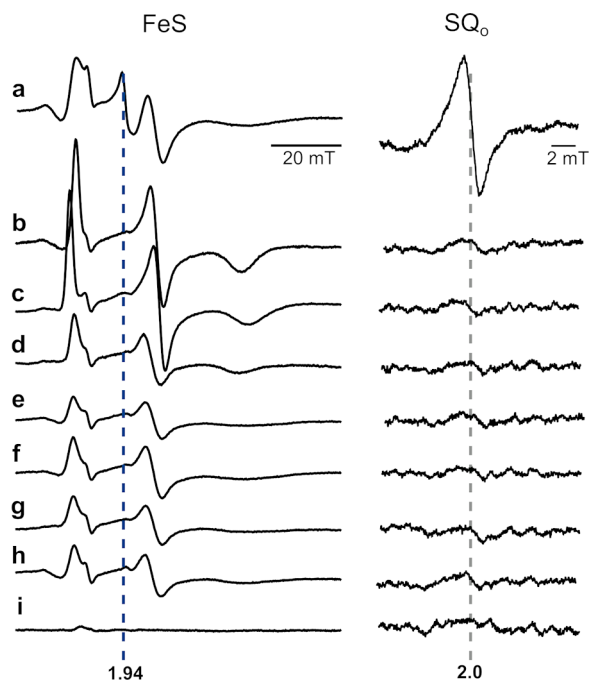


Figure 2. Testing the sensitivity of $g = 1.94$ and $g = 2.0$ signals to inhibitors and mutations that abolish the activity of the Q_o site. X-Band EPR spectra of isolated WT cytochrome bc_1 obtained under the conditions described for Figure 1c in the presence of antimycin alone (a) or antimycin and one of the Q_o site inhibitors: tridecyl-stigmatellin (b), atovaquone (c), famoxadone (d), myxothiazol (e), azoxystrobin (f), or kresoxim-methyl (g). Spectra of antimycin-inhibited mutants G158W (h) and the b_c -subcomplex (i). The left panel (FeS) shows spectra measured at 20 K in a magnetic field range of the FeS signal, and the right panel (SQ_o) shows spectra measured at 200 K in a magnetic field range typical of organic radicals.

<0.01 .^{29,31–34} The new $g = 1.94$ transition does not fall into this category, because the observed difference between the g_y of Rieske and the new signal was 1 order of magnitude larger ($\Delta g \sim 0.05$) and the signal disappeared over time. Most importantly, the $g = 1.94$ signal detected at X-band (9.46 GHz) shifted to a $g = 1.96$ when the same samples were

measured at Q-band (33.5 GHz) (Figure 3, black). This excludes the possibility that this signal originated from a new paramagnetic center. It thus must be a result of magnetic interactions between two closely separated paramagnetic species. An assumption that reduced FeS at the Q_o site is one of them leaves SQ_o as the only possible candidate for the other.

To verify that both FeS and SQ_o do interact with one another and to identify the dominant mechanism responsible for the appearance of a new EPR spectrum, we performed simulations based on a spin Hamiltonian including isotropic (scalar exchange) and anisotropic (exchange and dipolar) terms of spin coupling between SQ_o and the FeS cluster (Figure 3) (see details in the Supporting Information).¹⁸ Dipolar interaction alone appeared to be too weak to produce the $g = 1.94$ transition. However, when spin–spin exchange interaction was taken into account and its frequency $|J_0|$ was on the order of 3500 MHz ($\sim 0.1 \text{ cm}^{-1}$), the simulations neatly reproduced experimental spectra (Figure 3). We thus identified the SQ_o –FeS coupled system that at lower magnetic fields (those used at X-band) exists as a triplet state (and will be termed as such, in the remaining text). The SQ_o –FeS triplet emerges as a new intermediate of the reactions at the Q_o site that when formed averages the g transitions of SQ_o and FeS.

Distinct Population of SQ_o without Spin–Spin Exchange Interaction. The presence of a separate $g = 2.0$ SQ_o transition identified a distinct population of SQ_o centers for which spin–spin exchange with FeS does not exist or is too small to be resolved. Nevertheless, fast-relaxing paramagnetic metals of the Q_o site (oxidized heme b_L and reduced FeS) still exerted a profound impact on SQ_o , resulting in its unusually fast relaxation compared to the relaxation of chemically induced semiquinone in buffer (SQ_{CH}) or well-known Q_i site semiquinone (SQ_i).^{13,35} This manifested itself in significant homogeneous line broadening of the SQ_o signal (Figure 4a,b and Table 1), an inability to saturate it with microwaves (Figure 4c), and the presence of a Leigh effect (Figure 4d).²³ We note that the fast relaxation makes this SQ_o signal different from other reported SQ_o signals^{12,14,15} that did not show signs of interactions with the FeS and/or heme b_L metal centers of the Q_o site.

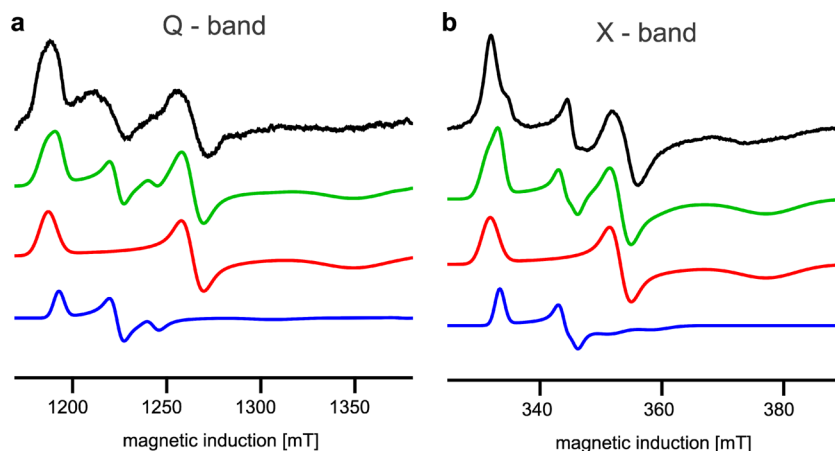


Figure 3. Simulating EPR spectra to define the physical nature of the $g = 1.94$ transition. Analysis of EPR transitions in a magnetic field range of the FeS signal at Q-band (a) and X-band (b) for the antimycin-inhibited +2Ala mutant. In panels a and b, experimental spectra (black) were simulated (green) as a sum of the FeS spectra (red) and the spectra resulting from exchange coupling between FeS and SQ_o (blue), assuming $|J_0| \sim 3500 \text{ MHz}$. Blue and red represent 17 and 83%, respectively, of the total number of spins in green. The blue spectrum in panel b represents the spectrum of the SQ_o –FeS triplet state.

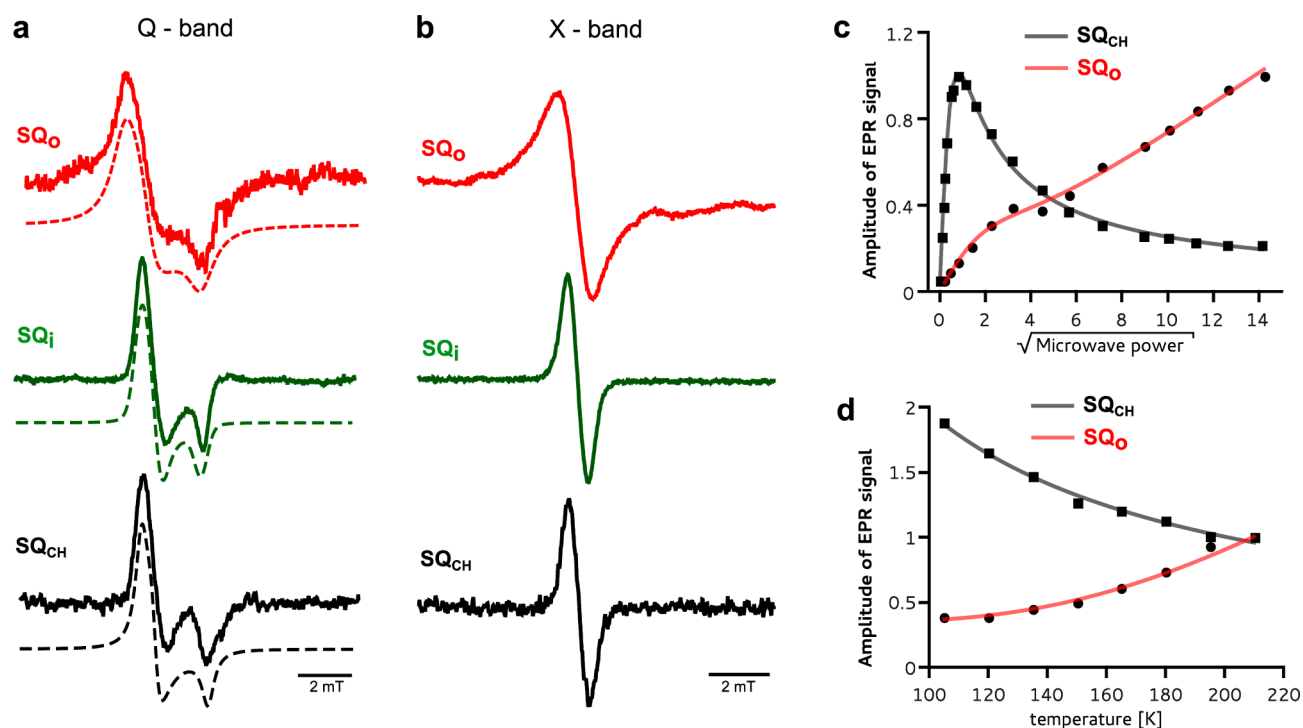


Figure 4. Unusual magnetic properties of the SQ_o center. (a) The Q-band spectrum of SQ_o (red) shows significant homogeneous broadening in comparison to the spectrum of SQ_i generated in myxothiazol-inhibited enzyme (green) or SQ_{CH} generated chemically in buffer (black). The spectra were simulated using the rhombic g tensor (dashed lines). (b) The same samples as in panel a measured at X-band. (c) X-band microwave power dependence of the amplitude of SQ_o at 200 K (red) compared with that of SQ_{CH} (black). (d) Temperature dependence of the SQ_o amplitude showing the Leigh effect (red) while SQ_{CH} obeys the Curie law (black). Solid lines in panels c and d represent appropriate fits (see Materials and Methods). a–d refer to the SQ_o signal generated in the +2Ala mutant for which the signal is the strongest (see Figure S2 of the Supporting Information).

Table 1. Parameters of Q-Band Semiquinone Spectra Obtained by Simulation

	g_z	g_y	g_x	homogeneous line broadening ^a (mT)
SQ_o	2.0059	2.0045	2.0010	0.718
SQ_i	2.0052	2.0043	2.0013	0.306
SQ_{CH}	2.0052	2.0043	2.0009	0.330

^aThe contribution from Gaussian broadening was set to 0.03 mT and kept constant in all simulations.

DISCUSSION

Conditions of Formation of SQ_o and SQ_o –FeS Coupled Centers Detected by EPR. In our experiments, the SQ_o –FeS coupled centers ($g = 1.94$) and SQ_o ($g = 2.0$) were detected during the continuous turnover of quinol oxidation and cytochrome c reduction when fast reoxidation of heme b_L through heme b_H and the Q_i site was prevented. Under such conditions, the reoxidation of heme b_L required to maintain the progress of oxidant-induced (by oxidized Rieske) heme b_L reduction is achieved by the transfer of an electron from heme b_L back to the Q_o site. Because the formation of the $g = 1.94$ signal requires the concomitant presence of the reduced FeS and SQ_o , the back electron transfer may predispose the Q_o site to generate the $g = 1.94$ signal if heme b_L reduces Q to form SQ_o (via semireverse reaction^{26–28}) at the time when reduced FeS is already present in the site.

Indeed, this appeared to be the dominant way through which the SQ_o –FeS triplet and SQ_o signals were trapped in our experiments. The first indication of that comes from the

observation that the signals were detected along with oxidized heme b_L (Figure 1c). Furthermore, the signals reached maximal amplitudes when FeS and cytochrome c (acting as the oxidizing pool) were approximately half-reduced (Figure 1b). This suggests that the probability of trapping the $g = 1.94$ and $g = 2.0$ intermediates comes as a result of competition between the rate of oxidant-induced heme b_L reduction and the rate of its oxidation by the transfer of an electron from heme b_L to Q to form SQ_o at the time when FeS is reduced. It follows that the conditions of the formation of SQ_o –FeS coupled centers are not favored at the beginning of the reaction, when the population of Rieske clusters is largely oxidized and capable of “consuming” electrons from SQ_o (time points before appearance of the $g = 1.94$ and $g = 2.0$ signals in Figure 1b). On the other hand, as the system reaches equilibrium, the populations of Rieske clusters and cytochrome c become largely reduced and the average oxidant-induced reduction of the heme b_L rate decreases, diminishing the amount of electron donor for Q at the Q_o site. This leads to the loss of SQ_o –FeS and SQ_o signals (Figure 1b).

Incorporation of the SQ_o –FeS Triplet State in the Electronic Reactions of the Q_o Site. Detection of the SQ_o –FeS triplet state along with the residual SQ_o sets a new stage for understanding the mechanism of reactions catalyzed by the Q_o site from both kinetic and thermodynamic points of view (Figure 5). It can be envisaged that the SQ_o –FeS triplet forms as an initial step of oxidation of QH_2 when oxidized FeS withdraws an electron from QH_2 (state b in Figure 5). Evolution of this state into the state where SQ_o and reduced FeS exist as separate spectral identities (state c in Figure 5)

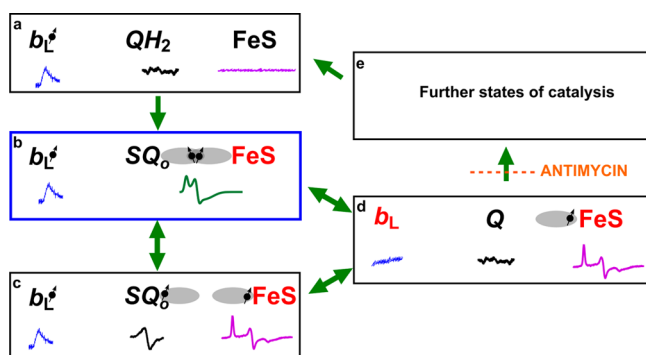


Figure 5. Model of electronic bifurcation of the Q_o site accommodating the SQ_o –FeS coupled system. (a) Bound QH_2 is flanked by oxidized heme b_L and oxidized FeS. (b) FeS withdraws an electron from QH_2 , which leads to the formation of the SQ_o –FeS triplet state. (c) The SQ_o –FeS distance increases (by movement of the FeS head domain and/or SQ_o), breaking spin exchange interaction, exposing separate spectra of SQ_o and reduced FeS. (d) Heme b_L is reduced by SQ_o generating Q . (e) In the noninhibited enzyme, heme b_L rapidly transfers an electron across the membrane to heme b_H directly or through heme b_L in the other monomer^{44,45} (not shown). The enzyme goes through further states to reach the initial state a. Antimycin prevents oxidation of heme b_H , interrupting the transition from state d to state e. Black and red denote the oxidized and reduced cofactor, respectively, while the dot with an arrow indicates the paramagnetic state of the center. Orbitals engaged in spin exchange are shown as gray ovals. Blue, black, magenta, and green spectra are EPR spectra of heme b_L , SQ_o , FeS, and the SQ_o –FeS triplet state, respectively. Green arrows show transitions between the enzyme states. The blue box denotes the state that was detected as a major fraction of SQ_o . The scheme does not consider the still unknown proton transfers that may influence transitions between the states.

leads to immediate reduction of heme b_L by SQ_o , which completes the reaction generating Q (state d in Figure 5). In this scheme, a direct transition from state b to state d cannot be ruled out and might be even rapid enough to consider the two-electron oxidation of QH_2 at the Q_o site as a virtually concerted process. The flow of electrons out from the cofactor chains (state e in Figure 5) allows the enzyme to regain state a to complete the cycle.

For this scheme, the measured $g = 1.94$ (the SQ_o –FeS triplet) and $g = 2.00$ (SQ_o) signals are spectroscopic signatures of states b and c, respectively. These states were detected only when the flow of electrons out from the Q_i site was blocked by antimycin (interrupted transition from state d to e) that, in the context of full reversibility of Q_o site reactions, indirectly increased the probability of transfer of an electron from reduced heme b_L to Q to form SQ_o (bringing the site back to state b or c).^{5,26–28}

One may ask why a significant amount of SQ_o cannot be detected in the noninhibited enzyme. At this stage, the precise answer is difficult. Nevertheless, we may propose that if electron transfer among SQ_o , heme b_L , and heme b_H is a pure tunneling process, not coupled to any chemical event (like protonation/deprotonation, conformational change, etc.), then freezing the samples will not prevent the transfer of the electron from SQ_o to heme b_H involving a transient step through heme b_L . However, in the antimycin-inhibited enzyme, heme b_H remains reduced; thus, in frozen samples containing a reduced FeS cluster, an electron may circulate only between SQ_o and heme b_L . Under these conditions, the highest probability of finding unpaired electrons is on SQ_o –FeS coupled centers, and

as long as the electron circulation is significantly slower than the Larmor frequency (~ 9.5 GHz), it exerts no effect on the EPR spectra of SQ_o –FeS coupled centers at the Q_o site.

Thermodynamic Properties of the SQ_o –FeS Couple.

While the quantity of residual SQ_o (from state c) cannot be determined because of the presence of the Leigh effect,²³ the estimated maximal abundance of the SQ_o –FeS triplet state (state b) reaches as much as ~ 9 and $\sim 17\%$ of the total concentration of FeS in WT and +2Ala cytochrome bc_1 , respectively (Figure 3). This indicates that SQ_o may not be as highly unstable as the models of the Q_o site assume.^{5,10,11,13} This raises the question of how much the stability constant (K_{stab}) of SQ_o detected in this work differs from the K_{stab} of $\ll 10^{-7}$ typically reported in the literature.^{7,14,15,25,36} Any temptations to estimate this difference must consider the fact that in our experiments the new intermediates were detected under nonequilibrium conditions of continuous turnover; thus, the use of K_{stab} for a description of the stability of SQ_o may be invalid, as this parameter is used to define stability in systems under thermodynamic equilibrium conditions. Nevertheless, the use of this parameter for the description of SQ_o –FeS triplet stability at the time point (t_{max}) where the amount of SQ_o is the highest yields a K_{stab} on the order of $10^{-2.6}$.⁴ This is more than 3 orders of magnitude larger than the previously defined upper limit of K_{stab} for SQ_o . Such a value of K_{stab} makes the stability of SQ_o comparable to stabilities of other semiquinones in proteins, such as that of the Q_i site.³⁵

Until now, the Q_o site has been considered exceptional in that, unlike other quinol oxidation–reduction sites, it did not stabilize semiquinones that were naturally volatile outside the protein matrix.² Our work suggests that the instability of SQ_o is apparent and is a consequence of the simultaneous accessibility of two redox partners rather than a lack of an influence of the site on the stability of SQ_o .

Relation of SQ_o to the Superoxide-Generating Activity of Cytochrome bc_1 . The observation that large quantities of SQ_o can be detected under aerobic conditions indicates that SQ_o is not as highly reactive with oxygen as current mechanisms of superoxide production by cytochrome bc_1 assume.^{10,11,14,37} In fact, high levels of the SQ_o –FeS triplet state signal observed in the +2Ala mutant, which does not produce any detectable superoxide,^{27,28} indicate that conditions of triplet formation (when SQ_o is likely to be hydrogen-bonded to histidine liganding the FeS cluster) do not impose a risk of electron leaks on oxygen. This, however, does not preclude the possibility that the enzyme faces such a risk if SQ_o is present at the time when FeS is remote from the Q_o site^{27,28} (and the hydrogen bond is not formed). This could be explained in analogy to the reactions of 1,4-semiquinones with oxygen in solution. In such chemical systems, it was found that “hydrogen bonding of the -OH moiety in the semiquinone radical to the HBA (hydrogen-bond-accepting) solvent prevents reaction of the semiquinone with O_2 .”³⁸

Possible Contribution of bc -Type Complexes to the $g = 1.94$ Signal in Other Bioenergetic Systems. Signals near $g = 1.94$ often reported in studies on mitochondrial and bacterial respiration have usually been attributed to iron–sulfur clusters of complex I and II, even though their origin was not always clear.^{39–42} Our work implies that the Q_o site of complex III, so far beyond consideration, should in fact be regarded as one of the possible contributors to the mitochondrial $g = 1.94$ signal. The diagnostic feature of the Q_o site-deriving $g = 1.94$ signal at X-band is its shift to larger values with an increase in

EPR frequency, as observed in cases of weak exchange between two paramagnetic centers.¹⁹ We anticipate that knowledge of spectroscopic properties of the SQ_o-FeS triplet signal will allow us to examine whether it can accumulate in mitochondria to relate SQ_o levels with other radicals, including ROS, formed during respiration.⁴³

CONCLUSIONS

In this work, we identify new EPR transitions ($g = 1.94$ and $g = 2.0$) associated with the enzymatic activity of cytochrome *bc*₁. Those two transitions revealed the presence of two distinct populations of semiquinone (SQ_o) formed at the quinol oxidation site (the Q_o site). The $g = 1.94$ signal was assigned as one of the transitions originating from SQ_o coupled to the Rieske cluster (FeS) by spin-spin exchange interaction. By analyzing the Q- and X-band EPR spectra of this coupled system, we estimated the 3500 MHz value of the isotropic exchange coupling constant, $|J_0|$, which is strong enough to create the SQ_o-FeS triplet state at the lower magnetic field typical of X-band. The radical signal centered at $g = 2.0$ corresponded to the population of fast-relaxing SQ_o for which spin-spin exchange does not exist or is too weak to be resolved. The paramagnetic properties of this signal were strongly affected by metal centers, consistent with its location between two fast-relaxing metal centers of the Q_o site (FeS and heme *b*_L). The detection of SQ_o together with oxidized heme *b*_L in samples containing antimycin suggests that the dominant way of generating SQ_o that can be detected under non-equilibrium conditions is the transfer of an electron from heme *b*_L to Q bound at the Q_o site. Under these conditions, the amount of SQ_o is comparable to the amount of stable semiquinones detected in catalytic sites of other bioenergetic enzymes.

ASSOCIATED CONTENT

Supporting Information

Simulations of EPR spectra, outline of catalytic cycle of cytochrome *bc*₁ (Figure S1), comparison of EPR spectra of wild type and +2Ala mutant (Figure S2) and references. This material is available free of charge via the Internet at <http://pubs.acs.org>.

AUTHOR INFORMATION

Corresponding Author

*E-mail: artur.osyczka@uj.edu.pl. Telephone: +48 12 664 63 48.

Funding

This work was supported by The Wellcome Trust International Senior Research Fellowship (to A.O.).

Notes

The authors declare no competing financial interest.

ABBREVIATIONS

SQ_o, semiquinone at the Q_o site; SQ_{CH}, chemically generated semiquinone; QH₂, ubihydroquinone; Q, ubiquinone; DBH₂, 2,3-dimethoxy-5-decyl-6-methyl-1,4-benzohydroquinone; EPR, electron paramagnetic resonance; FeS, two-iron, two-sulfur Rieske cluster; WT, wild type.

ADDITIONAL NOTE

^aGiven that ~20% of the total Rieske clusters is coupled to SQ_o, the total concentration of SQ_o is ~10 μM. This means

that the total concentrations of QH₂ and Q at t_{\max} are ~75 and ~580 μM, respectively. For these values, the K_{stab} calculated from the formula $K_{\text{stab}} = [\text{SQ}_o]^2 \times [\text{Q}]^{-1} \times [\text{QH}_2]^{-1}$ is $10^{-2.6}$.

REFERENCES

- (1) Holzenburg, A., and Scrutton, N. S., Eds. (2000) *Enzyme-Catalyzed Electron and Radical Transfer*, Kluwer Academic Publishers, New York.
- (2) Gunner, M. R., Madeo, J., and Zhu, Z. (2008) Modification of quinone electrochemistry by the proteins in the biological electron transfer chains: Examples from photosynthetic reaction centers. *J. Bioenerg. Biomembr.* 40, 509–519.
- (3) Mitchell, P. (1975) The protonmotive Q cycle: A general formulation. *FEBS Lett.* 59, 137–139.
- (4) Berry, E. A., Guergova-Kuras, M., Huang, L., and Crofts, A. R. (2000) Structure and function of cytochrome *bc* complexes. *Annu. Rev. Biochem.* 69, 1005–1075.
- (5) Osyczka, A., Moser, C. C., and Dutton, P. L. (2005) Fixing the Q cycle. *Trends Biochem. Sci.* 30, 176–182.
- (6) Zhang, H., Chobot, S. E., Osyczka, A., Wraight, C. A., Dutton, P. L., and Moser, C. C. (2008) Quinone and non-quinone redox couples in Complex III. *J. Bioenerg. Biomembr.* 40, 493–499.
- (7) Ding, H., Moser, C. C., Robertson, D. E., Tokito, M. K., Daldal, F., and Dutton, P. L. (1995) Ubiquinone Pair in the Q_o Site Central to the Primary Energy Conversion Reactions of Cytochrome *bc*₁ Complex. *Biochemistry* 34, 15979–15996.
- (8) Boveris, A., and Cadenas, E. (1975) Mitochondrial production of superoxide anions and its relationship to the antimycin insensitive respiration. *FEBS Lett.* 54, 311–314.
- (9) Muller, F., Crofts, A. R., and Kramer, D. M. (2002) Multiple Q-cycle bypass reactions at the Q_o site of the cytochrome *bc*₁ complex. *Biochemistry* 41, 7866–7874.
- (10) Cape, J. L., Bowman, M. K., and Kramer, D. M. (2006) Understanding the cytochrome *bc* complexes by what they don't do. The Q-cycle at 30. *Trends Biochem. Sci.* 11, 46–54.
- (11) Rutherford, A. W., Osyczka, A., and Rappaport, F. (2012) Back-reactions, short-circuits, leaks and other energy wasteful reactions in biological electron transfer: Redox tuning to survive life in O₂. *FEBS Lett.* 586, 603–616.
- (12) De Vries, S., Albracht, S. P. J., Berden, J. A., and Slater, E. C. (1981) A New Species of Bound Ubisemiquinone Anion in QH₂:Cytochrome *c* Oxidoreductase. *J. Biol. Chem.* 256, 11996–11998.
- (13) Junemann, S., Heathcote, P., and Rich, P. R. (1998) On the mechanism of quinol oxidation in the *bc*₁ complex. *J. Biol. Chem.* 273, 21603–21607.
- (14) Cape, J. L., Bowman, M. K., and Kramer, D. M. (2007) A semiquinone intermediate generated at the Q_o site of the cytochrome *bc*₁ complex: Importance for the Q-cycle and superoxide production. *Proc. Natl. Acad. Sci. U.S.A.* 104, 7887–7892.
- (15) Zhang, H., Osyczka, A., Dutton, P. L., and Moser, C. C. (2007) Exposing the complex III Q_o semiquinone radical. *Biochim. Biophys. Acta* 1767, 883–887.
- (16) Zhu, J., Egawa, T., Yeh, S.-R., Yu, L., and Yu, C.-A. (2007) Simultaneous reduction of iron-sulfur protein and cytochrome *b*_L during ubiquinol oxidation in cytochrome *bc*₁ complex. *Proc. Natl. Acad. Sci. U.S.A.* 104, 4864–4869.
- (17) Link, T. A. (1997) The role of the “Rieske” iron sulfur protein in the hydroquinone oxidation (Q_o) site of the cytochrome *bc*₁ complex. The “proton-gated affinity change” mechanism. *FEBS Lett.* 412, 257–264.
- (18) Fournel, A., Gambarelli, S., Guigliarelli, B., More, C., Asso, M., Chouteau, G., Hille, R., and Bertrand, P. (1998) Magnetic interactions between a [4Fe–4S]¹⁺ cluster and a flavin mononucleotide radical in the enzyme trimethylamine dehydrogenase: A high-field electron paramagnetic resonance study. *J. Chem. Phys.* 109, 10905–10913.
- (19) Calvo, R. (2007) EPR measurements of weak exchange interactions coupling unpaired spins in model compounds. *Appl. Magn. Reson.* 299, 271–299.

- (20) Valkova-Valchanova, M. B., Saribas, A. S., Gibney, B. R., Dutton, P. L., and Daldal, F. (1998) Isolation and Characterization of a Two-Subunit Cytochrome b-c₁ Subcomplex from *Rhodobacter capsulatus* and Reconstitution of Its Ubiquinol Oxidation (Q_o) Site with Purified Fe-S Protein Subunit. *Biochemistry* 37, 16242–16251.
- (21) Hyde, J. S., Pasenkiewicz-Gierula, M., Jesmanowicz, A., and Antholine, W. E. (1990) Pseudo Field Modulation in EPR Spectroscopy. *Appl. Magn. Reson.* 1, 483–496.
- (22) Altenbach, C., Froncisz, W., Hemker, R., McHaourab, H., and Hubbell, W. L. (2005) Accessibility of nitroxide side chains: Absolute Heisenberg exchange rates from power saturation EPR. *Biophys. J.* 89, 2103–2112.
- (23) Leigh, J. S. (1970) ESR Rigid-Lattice Line Shape in a System of Two Interacting Spins. *J. Chem. Phys.* 52, 2608–2612.
- (24) Stoll, S., and Schweiger, A. (2006) EasySpin, a comprehensive software package for spectral simulation and analysis in EPR. *J. Magn. Reson.* 178, 42–55.
- (25) Malnoë, A., Wollman, F.-A., De Vitry, C., and Rappaport, F. (2011) Photosynthetic growth despite a broken Q-cycle. *Nat. Commun.* 2, 1–6.
- (26) Dröse, S., and Brandt, U. (2008) The mechanism of mitochondrial superoxide production by the cytochrome bc₁ complex. *J. Biol. Chem.* 283, 21649–21654.
- (27) Borek, A., Sarewicz, M., and Osyczka, A. (2008) Movement of the iron-sulfur head domain of cytochrome bc₁ transiently opens the catalytic Q_o site for reaction with oxygen. *Biochemistry* 47, 12365–12370.
- (28) Sarewicz, M., Borek, A., Cieluch, E., Świerczek, M., and Osyczka, A. (2010) Discrimination between two possible reaction sequences that create potential risk of generation of deleterious radicals by cytochrome bc₁. Implications for the mechanism of superoxide production. *Biochim. Biophys. Acta* 1797, 1820–1827.
- (29) Czapl, M., Borek, A., Sarewicz, M., and Osyczka, A. (2012) Enzymatic activities of isolated cytochrome bc₁-like complexes containing fused cytochrome b subunits with asymmetrically inactivated segments of electron transfer chains. *Biochemistry* 51, 829–835.
- (30) Darrouzet, E., Valkova-Valchanova, M., Moser, C. C., Dutton, P. L., and Daldal, F. (2000) Uncovering the [2Fe-2S] domain movement in cytochrome bc₁ and its implications for energy conversion. *Proc. Natl. Acad. Sci. U.S.A.* 97, 4567–4572.
- (31) Cammack, R., Rao, K. K. K., and Hall, D. O. O. (1971) Effects of chaotropic agents on the spectroscopic properties of spinach ferredoxin. *Biochem. Biophys. Res. Commun.* 44, 8–14.
- (32) Sharp, R. E., Moser, C. C., Gibney, B. R., and Dutton, P. L. (1999) Primary steps in the energy conversion reaction of the cytochrome bc₁ complex Q_o site. *J. Bioenerg. Biomembr.* 31, 225–233.
- (33) Leggate, E. J., and Hirst, J. (2005) Roles of the Disulfide Bond and Adjacent Residues in Determining the Reduction Potentials and Stabilities of Respiratory-Type Rieske Clusters. *Biochemistry* 44, 7048–7058.
- (34) Zu, Y., Fee, J. A., and Hirst, J. (2002) Breaking and Re-Forming the Disulfide Bond at the High-Potential, Respiratory-Type Rieske [2Fe-2S] Center of *Thermus thermophilus*: Characterization of the Sulfhydryl State by Protein-Film Voltammetry. *Biochemistry* 41, 14054–14065.
- (35) Robertson, D. E., Prince, R. C., Bowyers, J. R., Katsumi, M., Dutton, P. L., and Ohnishi, T. (1984) Thermodynamic Properties of the Semiquinone and its Binding Site in the Ubiquinol-Cytochrome c (c₂) Oxidoreductase of Respiratory and Photosynthetic Systems. *J. Biol. Chem.* 259, 1758–1763.
- (36) Cape, J. L., Bowman, M. K., and Kramer, D. M. (2006) Understanding the cytochrome bc complexes by what they don't do. The Q cycle at 30. *Trends Plant Sci.* 11, 46–55.
- (37) Quinlan, C. L., Gerencser, A. a., Treberg, J. R., and Brand, M. D. (2011) The mechanism of superoxide production by the antimycin-inhibited mitochondrial Q-cycle. *J. Biol. Chem.* 286, 31361–31372.
- (38) Valgimigli, L., Amorati, R., Funo, M. G., DiLabio, G. A., Pedulli, G. F., Ingold, K. U., and Pratt, D. A. (2008) The unusual reaction of semiquinone radicals with molecular oxygen. *J. Org. Chem.* 73, 1830–1841.
- (39) Orme-Johnson, N. R., Hansen, R. E., and Beinert, H. (1974) Electron paramagnetic Resonance-detectable Electron Acceptors in Beef Heart Mitochondria. *J. Biol. Chem.* 249, 1928–1939.
- (40) Baker, J. E., Felix, C., Olinger, G. N., and Kalyanaraman, B. (1988) Myocardial ischemia and reperfusion: Direct evidence for free radical generation by electron spin resonance spectroscopy. *Proc. Natl. Acad. Sci. U.S.A.* 85, 2786–2789.
- (41) Shergill, J. K., Cammack, R., Chen, J.-H., Fisher, M. J., Madden, S., and Rees, H. H. (1995) EPR spectroscopic characterization of the iron-sulphur proteins and cytochrome P-450 in mitochondria from the insect *Spodoptera littoralis* (cotton leafworm). *Biochem. J.* 307, 719–728.
- (42) Iwasaki, T., Wakagi, T., and Oshima, T. (1995) Resolution of the Aerobic Respiratory System of the Thermoacidophilic Archaeon, *Sulfolobus* sp. Strain 7. *J. Biol. Chem.* 270, 30902–30908.
- (43) Murphy, M. P. (2009) How mitochondria produce reactive oxygen species. *Biochem. J.* 417, 1–13.
- (44) Lenciano, P., Lee, D.-W., Yang, H., Darrouzet, E., and Daldal, F. (2011) Intermonomer electron transfer between the low-potential hemes of cytochrome bc₁. *Biochemistry* 50, 1651–1663.
- (45) Świerczek, M., Cieluch, E., Sarewicz, M., Borek, A., Moser, C. C., Dutton, P. L., and Osyczka, A. (2010) An Electronic Bus Bar Lies in the Core of Cytochrome bc₁. *Science* 329, 451–454.